Article

Phosphoproteomics Screen Reveals Akt Isoform-Specific Signals Linking RNA Processing to Lung Cancer

Ioannis Sanidas,[1,5] Christos Polytarchou,[1,2,5] Maria Hatziapostolou,[1,2] Scott A. Ezell,[1,6] Filippos Kottakis,[1,7] Lan Hu,[3] Ailan Guo,[4] Jianxin Xie,[4] Michael J. Comb,[4] Dimitrios Iliopoulos,[2] and Philip N. Tsichlis[1,*]

[1]Molecular Oncology Research Institute, Tufts Medical Center, Boston, MA 02111, USA
[2]Division of Digestive Diseases, Center for Systems Biomedicine, David Geffen School of Medicine at UCLA, Los Angeles, CA 90095, USA
[3]Department of Biostatistics and Computational Biology, Center for Cancer Computational Biology, Dana-Farber Cancer Institute, Boston, MA 02215, USA
[4]Cell Signaling Technology, Danvers, MA 01923, USA
[5]These authors contributed equally to this work
[6]Present address: Cutaneous Biology Research Center, Massachusetts General Hospital and Harvard Medical School, Charlestown, MA 02129, USA
[7]Present address: Massachusetts General Hospital, Boston, MA 02114, USA
*Correspondence: ptsichlis@tuftsmedicalcenter.org
http://dx.doi.org/10.1016/j.molcel.2013.12.018

SUMMARY

The three Akt isoforms are functionally distinct. Here we show that their phosphoproteomes also differ, suggesting that their functional differences are due to differences in target specificity. One of the top cellular functions differentially regulated by Akt isoforms is RNA processing. IWS1, an RNA processing regulator, is phosphorylated by Akt3 and Akt1 at Ser720/Thr721. The latter is required for the recruitment of SETD2 to the RNA Pol II complex. SETD2 trimethylates histone H3 at K36 during transcription, creating a docking site for MRG15 and PTB. H3K36me3-bound MRG15 and PTB regulate *FGFR-2* splicing, which controls tumor growth and invasiveness downstream of IWS1 phosphorylation. Twenty-one of the twenty-four non-small-cell-lung carcinomas we analyzed express IWS1. More importantly, the stoichiometry of IWS1 phosphorylation in these tumors correlates with the *FGFR-2* splicing pattern and with Akt phosphorylation and Akt3 expression. These data identify an Akt isoform-dependent regulatory mechanism for RNA processing and demonstrate its role in lung cancer.

INTRODUCTION

Akt is an AGC family serine-threonine protein kinase. It is activated by a variety of extracellular and intracellular signals, and its activation depends on PtdIns-3,4,5-P3 and to a lesser extent on PtdIns-3,4-P2, both of which are products of the phosphoinositide 3-kinase (Franke et al., 1995; Manning and Cantley, 2007). Although the three Akt isoforms, Akt1, Akt2, and Akt3, have been treated by most of the earlier studies as a single entity, recent

evidence supports their unique roles in the regulation of cell function (Chen et al., 2001; Cho et al., 2001; Ezell et al., 2012; Iliopoulos et al., 2009; Maroulakou et al., 2007; Polytarchou et al., 2011; Tschopp et al., 2005; Wan et al., 2011).

To determine whether the functional differences between Akt isoforms are due to signaling differences, we employed a system of immortalized lung fibroblasts, which were engineered to express one Akt isoform at a time but are otherwise identical (Ezell et al., 2012; Iliopoulos et al., 2009; Polytarchou et al., 2011). A phosphoproteomics screen of these cells identified 606 proteins that are phosphorylated on Akt phosphorylation consensus sites in at least one of the Akt isoform-expressing cells. Analysis of the phosphoproteome data indeed identified signaling pathways and cellular functions preferentially regulated by one or another isoform. One of the differentially regulated functions was the posttranscriptional processing of mRNA (RNA metabolism) (Moore and Proudfoot, 2009).

One of the differentially phosphorylated proteins involved in the regulation of RNA metabolism is IWS1, which is phosphorylated at a conserved phosphorylation site, primarily by Akt3 and Akt1. IWS1 was originally identified in the yeast *Saccharomyces cerevisiae* through its interaction with Spt6 (Krogan et al., 2002), a histone H3/H4 chaperone (Duina, 2011). Spt6 also binds the C-terminal domain (CTD) of the large subunit of RNA Pol II, following the phosphorylation of the latter at Ser2 (Yoh et al., 2007). Recent studies in mammalian cells revealed that the Spt6/IWS1 complex contains two additional proteins: Aly/REF, an adaptor that contributes to nucleocytoplasmic RNA transport, and SetD2, a histone H3 trimethyl transferase (Yoh et al., 2007, 2008). The same studies showed that this complex contributes both to alternative RNA splicing and to nucleocytoplasmic RNA transport.

The regulation of RNA splicing is a complex and poorly understood process. Although some of the splicing events are constitutive, occurring in all cell types independently of external signals, others, also known as alternative splicing events, are conditional. Recent estimates suggest that at least 90% of the

metazoan genes are alternatively spliced (Wang et al., 2008). This gives rise to a proteome that is significantly more complex than the number of genes would suggest. Alternative splicing plays an important role in differentiation and development, as well as in the response of fully differentiated cells to various signals (Kalsotra and Cooper, 2011). Defects in alternative splicing have been linked to a host of human diseases, primarily neurodegenerative diseases and cancer (Cooper et al., 2009). Alternative splicing depends on the interplay of cis-acting RNA elements with trans-acting splicing factors (Chen and Manley, 2009), and on epigenetic cues, such as DNA methylation and histone modifications (Luco et al., 2011). However, very little is known about the control of this machinery by cellular signals (Zhou et al., 2012).

One of the genes that undergo alternative splicing during development and in some cancers is the gene encoding FGF Receptor-2 (FGFR-2) (Carstens et al., 2000; Warzecha et al., 2009). Alternative splicing gives rise to two isoforms of the receptor, the IIIc and the IIIb isoform, of which only the IIIc isoform is recognized by basic FGF (bFGF or FGF-2) (Miki et al., 1992). The IIIc isoform is expressed preferentially in mesenchymal cells, as opposed to epithelial cells (Luco et al., 2010; Orr-Urtreger et al., 1993), and promotes cell migration and invasiveness in response to FGF-2. Moreover, the FGFR-2 IIIb-to-IIIc switch has been linked to epithelial mesenchymal transition (EMT) and to a migratory and metastatic phenotype in cancer cells (Thiery and Sleeman, 2006). The FGFR-2 alternative splicing discussed above belongs to a subset of alternative splicing events which depend on histone H3 trimethylation at K36 in the body of the target gene and on the polypyrimidine tract binding protein (PTB) (Carstens et al., 2000; Luco et al., 2010).

The data presented in this report confirmed the differential phosphorylation of IWS1 at Ser720/Thr721 by Akt3 and Akt1 and showed that its phosphorylation at this site is required for the recruitment of SetD2 to the Spt6-IWS1-Aly/REF complex. In the absence of SetD2 recruitment to the complex in lung carcinoma cell lines, the trimethylation of histone H3 at K36 in the body of the FGFR-2 gene was impaired. This interfered with the recruitment of MRG15, an H3K36me3-binding protein, and its interacting partner PTB, and shifted the splicing of FGFR-2 from the IIIc to the IIIb isoform. The shift in the alternative splicing of FGFR-2 interferes with cell migration and invasiveness in response to FGF-2 and suppresses the proliferation and invasiveness of tumor cells both in culture and in animals. Addressing the expression of FGFR-2 in a set of lung-derived normal and tumor samples revealed that whereas the overall expression was similar in both, there was a shift toward the IIIc isoform in the tumor samples. More importantly, the relative expression of the IIIc and IIIb isoforms in non-small-cell-lung carcinomas (NSCLCs) correlated with the stoichiometry of IWS1 phosphorylation, and the latter correlated with Akt phosphorylation and Akt3 expression. Finally, data from "Oncomine" show that the levels of expression of IWS1 in lung cancer correlate with the tumor stage. These findings combined underpin the importance of this pathway in the pathogenesis of lung cancer. Overall, our data suggest that Akt isoform-dependent phosphorylation events are essential for RNA processing and provide insights into the role of Akt in carcinogenesis.

RESULTS

Differential Regulation of the Akt-Phosphoproteome by the Three Akt Isoforms

To investigate signaling differences between Akt isoforms, we performed a phosphoproteomics screen on an isogenic cellular platform, in which Akt null cells were engineered to express one Akt isoform at a time, or a combination of all three (Figure 1A and see Figure S1A available online). Cell lysates were digested with LysC, and the resulting peptides were affinity purified with Akt phosphosubstrate antibodies. Enriched phosphopeptides were digested with trypsin, purified over StageTip, and analyzed by mass spectrometry. Comparison of the Z scores (Figure S1B) of individual phosphorylation sites revealed significant differences between the phosphoproteomes of Akt1, Akt2, Akt3, and Akt1/2/3 cells (Figure 1B). To validate these data, we examined the Z scores of known phosphorylation events that were also detected in our screen (Figure 1C and Table S1), and we examined and confirmed a set of phosphorylation events first detected in the present study (Figures 1C and S1C–S1G). These analyses validated all phosphorylation events above MAD = -0.64. A Venn diagram of Akt1-, Akt2-, Akt3-, and Akt1/2/3-mediated phosphorylation events, with Z scores above MAD = 2, identified sets of proteins that are differentially phosphorylated by one or another isoform (Figure S2A). The subcellular localization of these proteins revealed differences in distribution between isoform-specific targets (Figure S2B). Moreover, bioinformatics analyses suggested that Akt isoforms differentially regulate canonical pathways and cell functions (Figures 2A and 2B). One of the functions predicted to be differentially regulated by different Akt isoforms is RNA metabolism, which is represented by 25 proteins that are involved in different stages of the process (Figures 3C and S2C).

Akt1 and Akt3 Phosphorylate IWS1 at Ser720/Thr721

One of the proteins we identified as a differentially phosphorylated Akt target was IWS1 (Figures 2D and 2E), which is known to contribute to the assembly of a transcriptional elongation complex on the Ser2-phosphorylated CTD of the large subunit of RNA polymerase II (Yoh et al., 2007, 2008). Immunoprecipitation of IWS1 from Flag-IWS1-transduced lung fibroblasts expressing Akt1, Akt2, or Akt3 with the Akt phosphosubstrate antibody and probing the immunoprecipitates with an anti-Flag antibody confirmed the Akt isoform-dependent phosphorylation of IWS1 at a site corresponding to the Akt phosphorylation consensus (Figure 2F). In agreement with this observation, the inhibition of all Akt activity in HELA cells with 5 μM of the Akt inhibitor MK2206 blocked IWS1 phosphorylation (Figure 2G). Finally, in vitro kinase assays using bacterially expressed wild-type IWS1 and its phosphorylation site mutants as substrates confirmed that IWS1 is phosphorylated directly by Akt and that Ser720/Thr721 is the only Akt phosphorylation site in this protein (see Supplemental Information for further discussion). Remarkably, IWS1 was phosphorylated by Akt3 and less efficiently by Akt1, but not Akt2, suggesting that isoform-dependent phosphorylation specificity may be the result of structural differences that directly affect substrate recognition (Figures 2H and S2D).
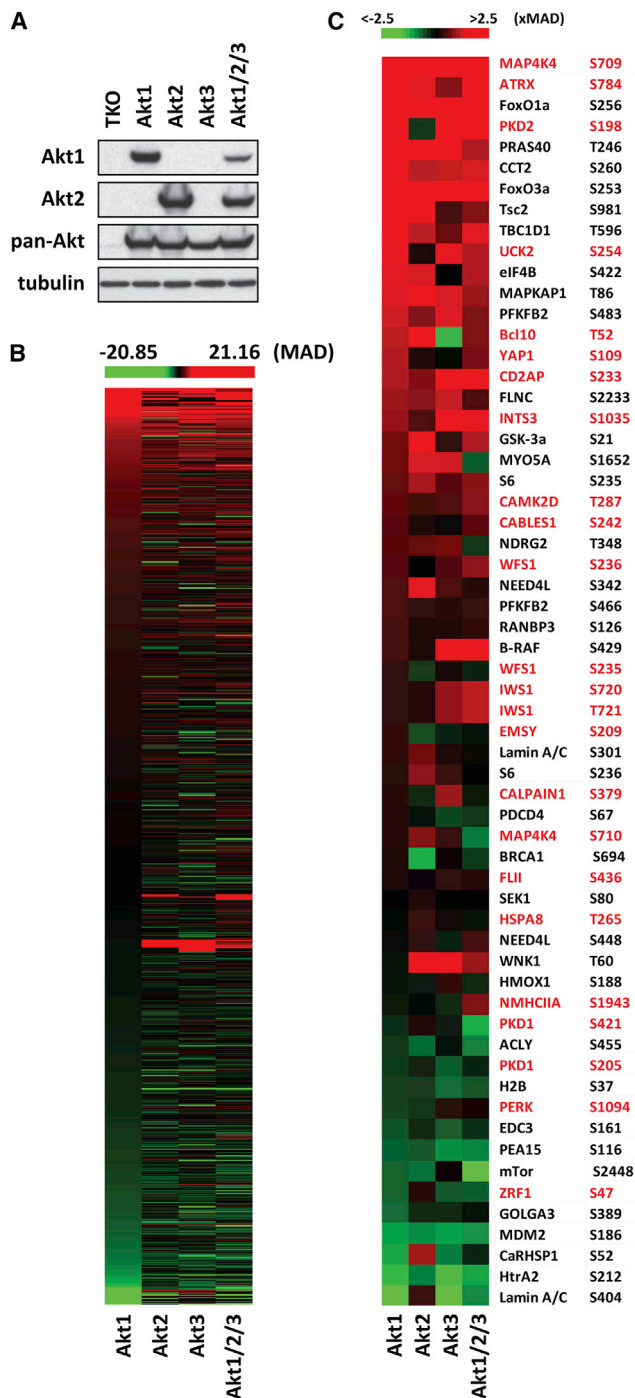
Figure 1. The Phosphoproteomes of Akt1-, Akt2-, Akt3-, and Akt1/2/3-Expressing Cells

(A) Western blots of cell lysates of Akt null (TKO) lung fibroblasts and their Akt isoform-expressing derivatives were probed with the indicated antibodies.

(B) Heatmap of the relative abundance of all the phosphorylation events detected in the phosphoproteomics screen. The relative abundance of each phosphorylation event is presented as the robust Z score of the ratio Akt1/TKO, Akt2/TKO, Akt3/TKO, or Akt1/2/3/TKO.

(C) Heatmap of the abundance of phosphorylation of known Akt substrates (black) and Akt substrates that were identified in this screen (red). The phosphorylated residue is shown on the right.

IWS1 Phosphorylation at Ser720/Thr721 Is Required for the Recruitment of SetD2 to the RNA Polymerase II Elongation Complex

To determine the biological significance of IWS1 phosphorylation, we first examined its expression in a set of human tumor cell lines. This analysis identified the NSCLC cell lines NCI H522 and NCI H1299 as high expressors and T47D, a human mammary carcinoma cell line, as a low expressor (Figure S3A). Western blotting confirmed that NCI H522 and NCI H1299 cells express higher levels of IWS1 than T47D cells. IGF1 stimulation of these cells revealed that IWS1 phosphorylation is regulated by receptor tyrosine kinase-generated signals and correlates with activation of Akt (Figure 3A).

In parallel experiments NCI H522, NCI H1299, and T47D cells were transduced with shIWS1-resistant constructs of FLAG-IWS1 or Flag-IWS1S720A/T721A. Subsequent infection of these cells with the shIWS1 lentiviral construct gave rise to cell lines in which the endogenous IWS1 was knocked down or replaced by exogenous wild-type or mutant IWS1 (Figure 3B). The phosphorylation of the wild-type protein was confirmed by probing IWS1 immunoprecipitates of wild-type and mutant rescue cell lysates with the Akt phosphosubstrate antibody (Figure 3C, upper panel). Alternatively, lysates from the same cells were probed with the phospho-IWS1 and total IWS1 antibodies (Figure 3C, lower panel). The specificity of the phospho-IWS1 antibody was further validated by using it to probe lysates of NCI H1299 and T47D cells, before and after treatment with MK2206 (Figure S3B).

IWS1 interacts with Spt6, which binds the phosphorylated Ser2 in the CTD of RNA Pol II, Aly/REF, and SetD2 (Yoh et al., 2007, 2008). Coimmunoprecipitation experiments revealed that the Ser720/Thr721 phosphorylation mutant of IWS1 fails to bind SetD2 but continues to bind Aly/REF and SPT6. As a result, neither IWS1 nor RNA Pol II coimmunoprecipitates with SetD2 (Figure 3D). This finding was confirmed with the reciprocal immunoprecipitation experiment. An HA-SetD2 construct was introduced into shIWS1 NCI H1299 cells rescued with wild-type or mutant IWS1. FLAG-IWS1 was immunoprecipitated from cells rescued with wild-type IWS1, before and after treatment with MK2206, as well as from cells rescued with mutant IWS1, and western blots of the immunoprecipitates were probed with an anti-HA antibody. The results (Figure S3C) confirmed the data in Figure 3D.

SetD2 catalyzes the trimethylation of histone H3 at K36, a histone mark linked to alternative splicing of a set of genes that include *FGFR-2* (Kolasinska-Zwierz et al., 2009; Luco et al., 2010). Alternative splicing via an H3K36me3-regulated process (Luco et al., 2010) gives rise to the *FGFR-2* isoforms IIIb and IIIc (Figure 3E), which encode receptors with different ligand specificities and different expression patterns (Luco et al., 2010; Miki et al., 1992). Replacement of endogenous IWS1 with its phosphorylation site mutant prevented the binding of SetD2 and decreased the abundance of histone H3K36me3 in the *FGFR-2* gene. Chromatin immunoprecipitations (ChIPs) revealed that IWS1 binds to exons IIIb and IIIc, but not to the transcription start site (TSS) of *FGFR-2* (Figure 3F), and that IWS1 phosphorylation at Ser720/Thr721 is not required for the binding (Figures 3G and S3D). ChIP assays for SetD2 in cells transduced
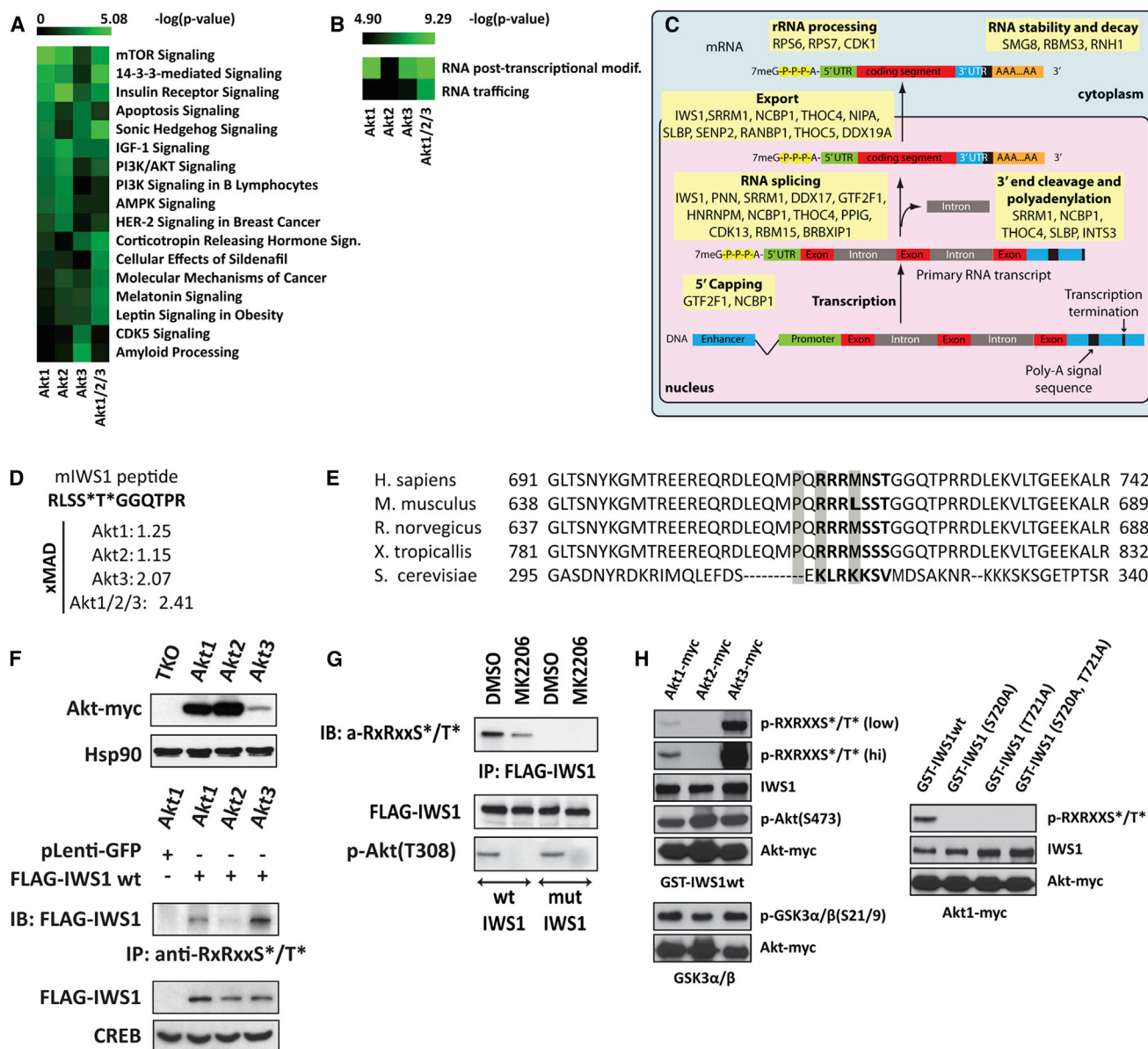
Figure 2. The Phosphoproteomes of Akt1-, Akt2-, and Akt3-Expressing Cells Suggest Functional Differences between Akt Isoforms; IWS1 Phosphorylation by Akt1 and Akt3

(A) Heatmap showing the probability [−log(p value)] that a given canonical pathway may be regulated by Akt1, Akt2, Akt3, or Akt1/2/3. Analysis based on phosphorylation events with a robust Z score ≥2 MAD.

(B) Probability that RNA trafficking and RNA posttranscriptional modifications may be regulated by Akt1, Akt2, or Akt3.

(C) Diagram of the sequential steps involved in RNA processing. Akt targets identified or confirmed by our screen are indicated.

(D) Sequence of the phosphorylated IWS1 peptide. The asterisks show the phosphorylated residues. The numbers show the median absolute deviation of the robust Z scores.

(E) Conservation of the phosphorylated peptide and the adjacent sequence.

(F) (Upper) Western blots of TKO lung fibroblasts and their Akt isoform-expressing derivatives were probed with anti-myc or anti-Hsp90 (loading control). (Lower) The lung fibroblasts in the upper panel were transduced with the indicated constructs, and their lysates were used for immunoprecipitation and immunoblotting with the indicated antibodies. Western blots of the same lysates were probed with anti-FLAG or anti-CREB, as indicated.

(G) HeLa cells transduced with lentiviral constructs of FLAG-IWS1 (WT or mutant) were treated with 5 μM MK2206 or DMSO for 2 hr. Anti-Flag-IWS1 immunoprecipitates were probed with the Akt phosphosubstrate antibody. Western blots of the same cell lysates were probed with the indicated antibodies.

(H) (Left) In vitro kinase assays of myc-tagged Akt1, Akt2, or Akt3, using GST-IWS1wt (upper panel) and GSK3α/β (lower panel) recombinant proteins as substrates. Phosphorylation was detected with the Akt phosphosubstrate or the phospho-GSK3α/β (21/9) antibody. (Right) In vitro kinase assay of myc-Akt1 using WT or mutant GST-IWS1 as substrates.

with an HA-SetD2 construct confirmed that IWS1 phosphoryla-tion is required for SetD2 recruitment to the *FGFR-2* gene (Fig-ures 3H, 3I, and S3E) and the trimethylation of histone H3 at K36 in exons IIIb and IIIc (Figures 3J and 3K).

IWS1 Phosphorylation at Ser720/Thr721 Regulates the Alternative Splicing of *FGFR-2*

High abundance of histone H3K36me3 in the IIIb exon is a signal for exon skipping, while low abundance of the same mark is a signal for exon inclusion (Kolasinska-Zwierz et al., 2009). As a result, knocking down SetD2 or IWS1, which is required for the recruitment of SetD2 to the elongation complex, increased the abundance of the IIIb relative to the IIIc tran-scripts, in NCI H522 and NCI H1299 cells, which express primarily *FGFR-2* IIIc, but not in T47D cells, which express primarily *FGFR-2* IIIb (Figures 4A, 4B, S4A, and S4B). More importantly, the change in alternative splicing induced by the knockdown of IWS1 was rescued by the wild-type IWS1, but not by IWS1S720A/T721A (Figure 4B). We conclude that IWS1 phosphorylation by Akt3 and Akt1 shifts the balance of *FGFR-2* splicing toward *FGFR-2*-IIIc, by regulating the recruit-ment of SetD2 to the elongation complex. If the recruitment of SetD2 depends on the phosphorylation of IWS1, as our data indicate, one would expect that overexpression of SetD2 would not rescue the *FGFR-2* alternative splicing phenotype in shIWS1 and shIWS1/mutant rescue cells. The experiment in Figure S4C confirmed the prediction.

To address the dependence of *FGFR-2* alternative splicing on Akt, we treated the cells with 5 μM MK2206, a dose that fully inhibits all Akt isoforms. Akt inhibition reduced H3K36 trimethy-lation in exons IIIb and IIIc and promoted exon IIIb inclusion in the *FGFR-2* transcript (Figure 4C), suggesting that the IWS1 phosphorylation phenotype depends on the activity of Akt. Knocking down different Akt isoforms sequentially or in combi-nation in the same cells not only confirmed this conclusion but also showed that the skipping of exon IIIb is promoted primarily by Akt3 and Akt1 (Figure 4D).

The preceding data raised the question of whether Akt regu-lates *FGFR-2* splicing primarily by phosphorylating IWS1 or whether it also utilizes an alternative pathway. To address this question, we examined the splicing of *FGFR-2* in MK2206 or DMSO-treated NCI H522 and NCI H1299 cells transduced with the phosphomimetic mutant IWS1-S720D/T721E (IWS1-DE) or with the empty vector (EV). The results showed that IWS1-DE rescues the MK2206-induced *FGFR-2* alternative splicing phenotype (Figure 4E). The rescue of the MK2206-induced shift in alternative splicing by the Akt-independent IWS1-DE mutant supports the hypothesis that Akt controls *FGFR-2* alternative splicing by phosphorylating IWS1, and not through an alternative pathway. Support for this conclusion was provided by the exper-iment in Figure S4D, which showed that none of the Akt isoforms can reverse the shIWS1- or shSetD2-induced shifts in *FGFR-2* splicing when overexpressed in NCI H522 cells. Although this conclusion is in agreement with all the data in this report, it should be viewed with caution, because Akt overexpression had no effect on *FGFR-2* alternative splicing even in shControl cells (Figure S4D), perhaps because NCI H522 cells express suf-ficient levels of Akt to keep the pathway fully active.

If IGF1 promotes the phosphorylation of IWS1, perhaps through Akt (Figure 3A), and the phosphorylation of IWS1 shifts the alternative splicing of *FGFR-2* toward the IIIc isoform, one would expect that treatment of NCI H522 and NCI H1299 cells with IGF1 would decrease the *FGFR-2* IIIb/IIIc ratio. The experi-ment in Figure 4F confirmed this prediction and provided evi-dence that Akt regulates *FGFR-2* alternative splicing by receptor tyrosine kinase-induced signals.

IWS1 Phosphorylation at Ser720/Thr721 Is Required for the Binding of MRG15 and PTB to the *FGFR-2* Gene

Histone H3K36me3 provides a docking site for MRG15 (Zhang et al., 2006), a chromodomain protein that interacts with the polypyrimidine track binding protein (PTB) to translate the H3K36me3 mark into a signal that regulates alternative splicing (Luco et al., 2010). Consistent with the data on SetD2 binding and histone H3K36 trimethylation in the *FGFR-2* gene (Figure 3), chromatin IPs in NCI H522 and NCI H1299 cells confirmed that knocking down IWS1 reduces the binding of both MRG15 and PTB and that their binding is restored by wild-type, but not the mutant IWS1 (Figures 4G, 4H, 4I, 4J, and S4E).

The data in Figure 4C confirmed that the regulation of FGFR-2 alternative splicing by SetD2 is IWS1 phosphorylation depen-dent. Since the binding of MRG15 and PTB to target genes de-pends on histone H3K36 trimethylation, which is mediated by SetD2, these data suggest that MRG15 and PTB would also regulate *FGFR-2* alternative splicing in an IWS1 phosphoryla-tion-dependent manner. This prediction was confirmed with the experiment in Figure S4F, which showed that the MK2206-induced increase in the IIIb/IIIc ratio is not rescued by MRG15, PTB, or SetD2. We conclude that the regulation of *FGFR-2* alter-native splicing by SetD2, MRG15, and PTB is strictly dependent on IWS1 phosphorylation by Akt.

Model of the Regulation of PTB-Dependent Alternative Splicing by IWS1 Phosphorylation

Based on the data presented in Figure 3 and Figure 4, we propose that IWS1 phosphorylation regulates PTB-dependent alternative splicing via the mechanism described in the model in Figure 5. According to this model, IWS1 phosphorylation is required for the recruitment of SetD2 to RNA Pol II. Inhibition of IWS1 phosphorylation prevents the trimethylation of histone H3 at K36 in the body of *FGFR-2* and perhaps other target genes. This abrogates the recruitment of the histone H3K36me3-inter-acting protein MRG15 and its binding partner PTB and results in shifts in alternative splicing of target genes, such as *FGFR-2*.

Alternative Splicing of *FGFR-2* Induced by IWS1 Phosphorylation at Ser720/Thr721 Promotes Cell Migration, Invasiveness, and Proliferation in Response to FGF-2

The IIIb isoform of *FGFR-2* is not recognized by FGF-2 (bFGF) whereas the IIIc isoform is (Miki et al., 1992). This suggested that by shifting *FGFR-2* splicing from the IIIb to the IIIc isoform, the Akt1/Akt3-dependent IWS1 phosphorylation would promote cell migration and proliferation in response to FGF-2. Wound healing and transwell filter assays in NCI H1299 and NCI H522 cells confirmed that IWS1 phosphorylation indeed promotes
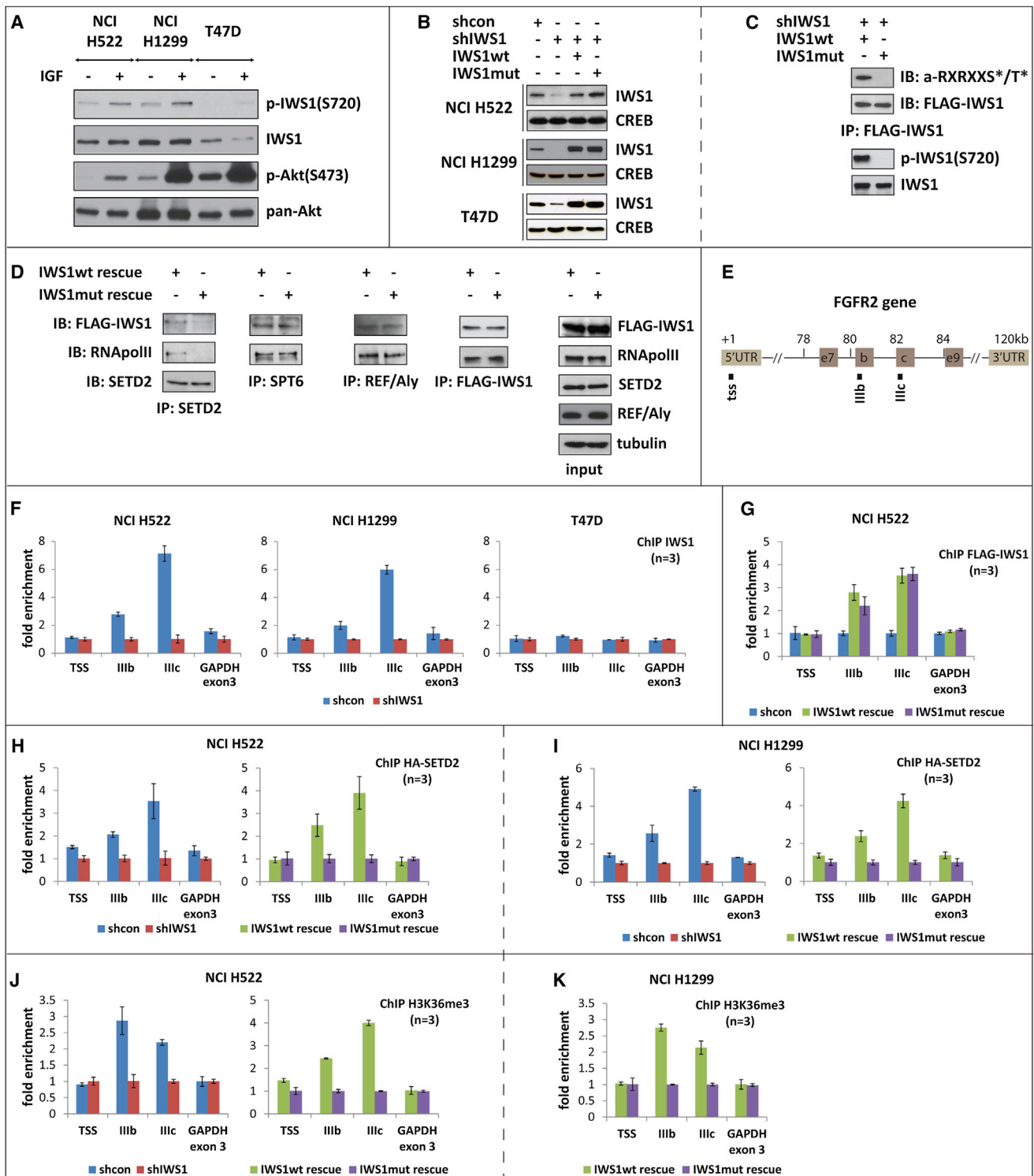
Figure 3. IWS1 Phosphorylation at Ser720/Thr721 Is Required for SETD2 Recruitment and H3K36me3 Trimethylation in the *FGFR-2* Gene

(A) NCI H522, NCI H1299, and T47D cell lysates, harvested before and after treatment with IGF-1, were probed with the indicated antibodies.

(B) Lysates of shControl, shIWS1, shIWS1/WT rescue and shIWS1/mutant rescue NCI H522, NCI H1299, and T47D cells were probed with the indicated antibodies.

(C) (Upper) Flag-IWS1 immunoprecipitates of shIWS1/WT rescue and shIWS1/mutant rescue NCI H1299 cells were probed with the Akt phosphosubstrate or the anti-FLAG (IWS1) antibody. (Lower) The same lysates were probed with antibodies to phospho-IWS1 or total IWS1.

(legend continued on next page)

both nondirectional and directional cell migration in the presence of FGF-2 (Figures 6A, 6B, S5A, and S5C). Similarly, matrigel invasion and cell proliferation assays confirmed that IWS1 phosphorylation promotes cell invasion and proliferation downstream of FGF-2 (Figures 6C, S5B, S5C, and 6D). To determine whether the expression of the IIIc, as opposed to the IIIb isoform of *FGFR-2*, is responsible for the enhanced migration and proliferation of the shControl and the shIWS1/WT rescue cells, we infected shIWS1-transduced NCI H1299 cells with constructs expressing the IIIc or IIIb isoforms. shControl and shIWS1 cells not transduced with the IIIc or IIIb construct were used as controls. Using these cells we showed that whereas the expression of the IIIc isoform rescues fully the impaired migration and invasiveness of cells growing in FGF-2-supplemented media (Figures 6E, 6F, and 6G), the expression of the IIIb isoform does not (Figures 6I, 6J, and 6K). The IIIc isoform also rescued the impaired proliferation phenotype of the same cells, although only partially (Figure 6H). A repeat of the cell proliferation experiment in cells growing in DMEM supplemented with 10% serum revealed that cell proliferation under these conditions is also regulated by IWS1 phosphorylation at Ser720/Thr721 (Figures 6L, 6M, and 6N). Despite that, *FGFR-2* IIIc overexpression did not rescue the impaired proliferation induced by IWS1 knockdown (Figure S5D), suggesting that although IWS1 phosphorylation regulates the proliferation of cells growing both in FGF-2 and in serum-supplemented media, the mechanisms by which it functions in the two culture conditions are not the same. Thus, whereas IWS1 phosphorylation regulates cell proliferation of cells growing in FGF-2-supplemented media in part by shifting the alternative splicing pattern of *FGFR-2*, in cells growing in serum-supplemented media it may function by regulating the transcriptional elongation or splicing of other target genes.

Experiments in Figures S4C and S4F showed that overexpression of SetD2 in NCI H522 and NCI H1299 cells cannot rescue the FGFR-2 splicing defect induced by blocking the IWS1 phosphorylation or by inhibiting the activity of Akt. These data predict that SetD2 should not rescue the impaired migration and invasiveness phenotype in cells in which the expression or phosphorylation of IWS1 was blocked. The experiments in Figure S5E confirmed the prediction. Given our observation that the splicing phenotype of the IWS1 phosphorylation block is not affected by SetD2 overexpression, it is unlikely that it will be affected by MRG15 or PTB. However, the overexpression

of these molecules may affect the biological phenotype, because they may have additional activities unrelated to RNA splicing.

The Role of IWS1 Phosphorylation at Ser720/Thr721 in Lung Cancer

To determine the role of IWS1 phosphorylation in oncogenesis, shControl, shIWS1, shIWS1/WT rescue, and shIWS1/mutant rescue NCI-H1299 cells were injected subcutaneously in nude mice. The inoculated animals were monitored for tumor growth, and they were sacrificed 4 weeks later. The results confirmed that IWS1 phosphorylation promotes both the growth and invasiveness of the tumor cells (Figures 7A and S6A). Immunohistochemical analysis of the xenografts with the validated anti-phospho-IWS1 antibody (Figures 3C and S3B) confirmed the IWS1 phosphorylation in vivo (Figure 7B).

Western blotting of cell lysates derived from a set of human lung specimens (2 normal and 24 NSCLCs) revealed that IWS1 is not expressed in normal lung but is expressed in 21 of 24 NSCLCs (Figure 7D). Immunohistochemical staining of a normal lung and NSCLC tissue array (17 and 23 samples, respectively) with the anti-phospho-IWS1 antibody also revealed increased phospho-IWS1 nuclear staining in a fraction of the tumors (Figure S6B). Based on these findings, which suggest a potential role for IWS1 in NSCLC, we proceeded to address the expression of *FGFR-2* IIIb and IIIc in normal lung and NSCLC samples. The results revealed that the overall *FGFR-2* expression is similar in both, but it shifts toward IIIc in the tumor samples (Figure 7C). More importantly, the shift correlates with the phosphorylation of IWS1, and the latter correlates with the phosphorylation of Akt and the expression of Akt3. Plotting the relative stoichiometry of IWS1 phosphorylation (p-IWS1-(S720)/total IWS1) against the *FGFR-2* IIIb/IIIc ratio in the 21 NSCLC samples that express IWS1 revealed that whereas tumors with high relative levels of IWS1 phosphorylation have almost universally low IIIb/IIIc ratios, tumors with low relative levels of IWS1 phosphorylation exhibit IIIb/IIIc ratios that are randomly distributed (Figures 7D and 7E) ($p = 0.0002$, by Levene's test for equality of variances). Plotting the relative stoichiometry of IWS1 phosphorylation against phospho-Akt (Ser 473), or Akt3 (Figure 7E), also revealed statistically significant correlations ($p = 0.00636$ and $p = 0.00745$, respectively, by Spearman's rank order correlation). Collectively, these data provide strong support to the hypothesis that the

(D) SetD2, Spt6, REF/Aly, and Flag-IWS1 immunoprecipitates from lysates of shIWS1/WT rescue and shIWS1/mutant rescue NCI H522 cells were probed with anti-Flag (IWS1), anti-RNA PolII, and antiSetD2, as indicated. The same cell lysates were probed with the indicated antibodies.

(E) Schematic showing the alternatively spliced exons 8 (IIIb) and 9 (IIIc) of the human *FGFR-2* gene. The map position of the primer sets is indicated by square dots. TSS, transcription start site.

(F) ChIP assays showing the binding of IWS1 to the *FGFR-2* and GAPDH genes in the indicated shControl and shIWS1 cells. Bars show the mean fold enrichment in the binding of endogenous IWS1 in shControl, versus shIWS1 cells ± SD.

(G) ChIP of Flag-IWS1 in shIWS1/WT rescue and shIWS1/mutant rescue NCI H522 cells shows that both WT and mutant IWS1 bind exons IIIb and IIIc of *FGFR-2*. Bars show the mean fold enrichment in binding of Flag-IWS1 in these cells, relative to the parental cells ±SD. IWS1 binding is also presented as percentage of the input in Figure S3D.

(H and I) ChIP assays showing the binding of HA-SetD2 to the *FGFR-2* and *GAPDH* genes in the indicated shControl, shIWS1, shIWS1/WT rescue, and shIWS1/ mutant rescue cells, transduced with an HA-SetD2 lentiviral construct. Bars show the mean fold enrichment in binding of HA-SetD2 in shControl relative to shIWS1 cells or in shIWS1/WT rescue relative to shIWS1/mutant rescue cells ±SD. HA-SetD2 expression and binding are also presented as percentage of the input in Figure S3E.

(J and K) ChIP assays showing the abundance of histone H3K36me3 in the *FGFR-2* and *GAPDH* genes in the indicated cells. Bars show the mean fold enrichment in H3K36me3 in shControl relative to shIWS1 cells or in shIWS1/WT rescue relative to shIWS1/mutant rescue cells ±SD.
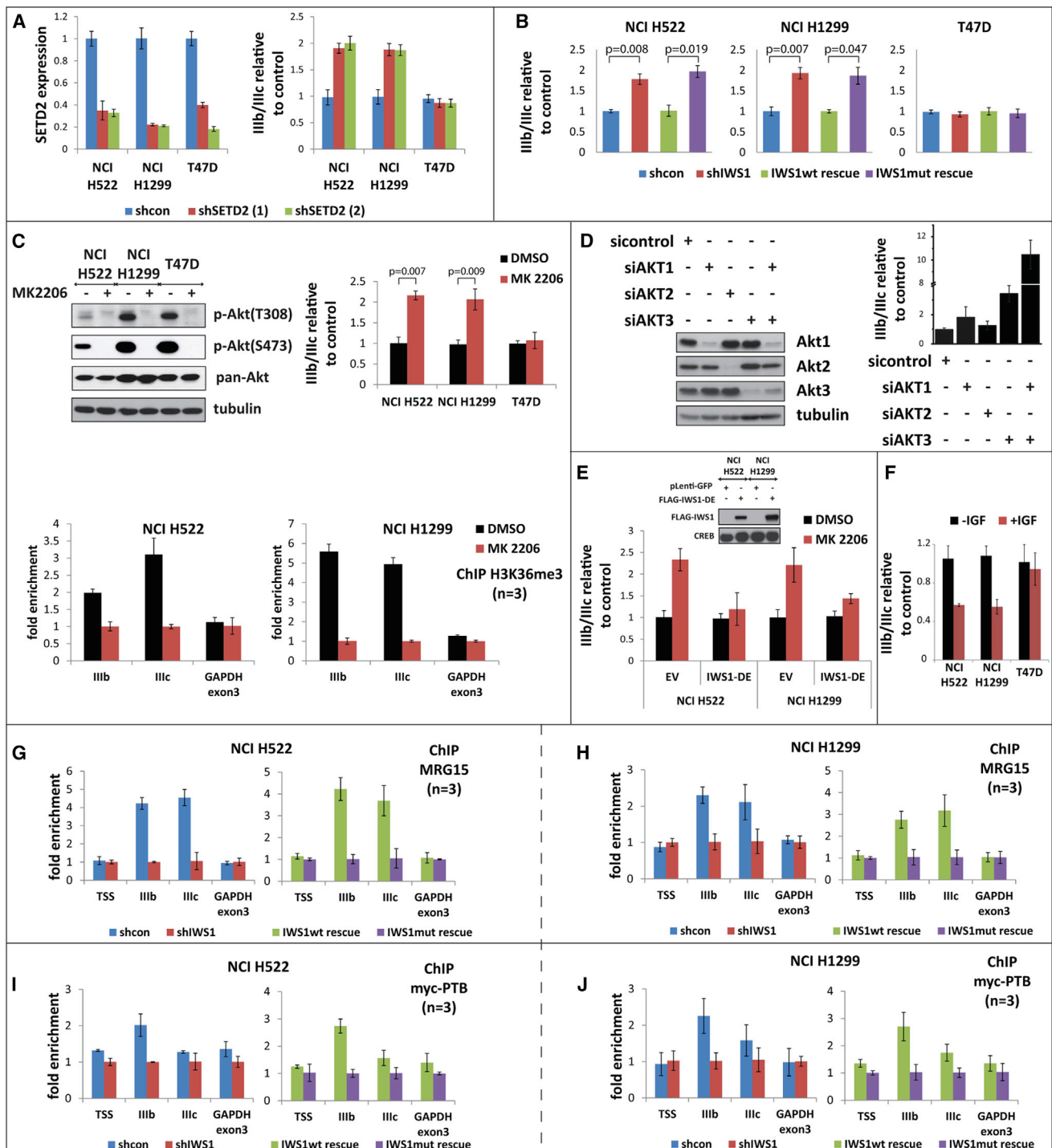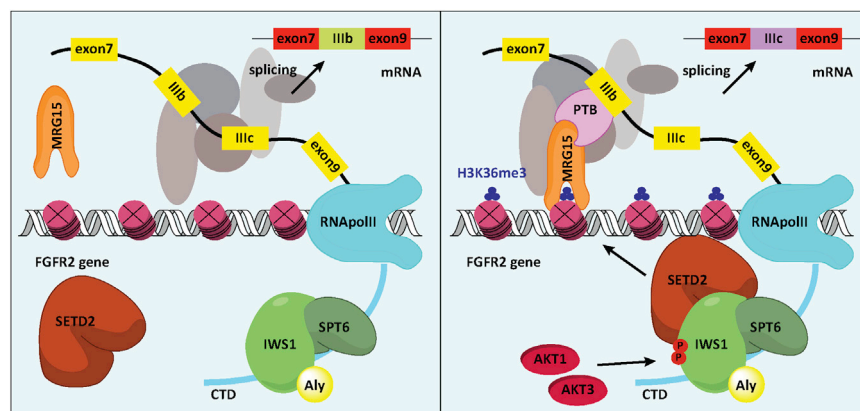
Figure 4. IWS1 Phosphorylation at Ser720/Thr721 by Akt3 and Akt1 Regulates the Alternative Splicing of the *FGFR-2* Gene

(A) The SETD2 knockdown shifts the IIIb/IIIc ratio of the *FGFR-2* mRNA toward the IIIb isoform. (Left) Real-time RT-PCR for *SETD2* in the indicated cell lines transduced with two different shSetD2 constructs or with an shControl construct. (Right) Real-time RT-PCR showing the IIIb/IIIc *FGFR-2* mRNA ratios in the cells on the left panel. Bars show the mean *SETD2* levels or the mean IIIb/IIIc ratios in shSetD2, relative to shControl cells ±SD.

(B) IWS1 phosphorylation regulates *FGFR-2* alternative splicing. Real-time RT-PCR showing the IIIb/IIIc *FGFR-2* ratios in the indicated shControl, shIWS1, shIWS1/WT rescue, and shIWS1/mutant rescue cells. Bars show the mean IIIb/IIIc ratio in shIWS1, shIWS1/WT rescue, and shIWS1/mutant rescue cells relative to shControl cells ±SD.

(C) Akt inhibition interferes with histone H3K36 trimethylation in the *FGFR-2* gene and promotes inclusion of the IIIb exon in the transcript. (Top left) Lysates of the indicated cells, harvested before and after a 2 hr treatment with MK2206 (5 μM) or DMSO, were probed with antibodies, as shown. (Top right) The *FGFR-2* IIIb to

(legend continued on next page)

Figure 5. Model of the Regulation of *FGFR-2* Alternative Splicing by IWS1 Phosphorylation at Ser720/Thr721 by Akt1 or Akt3

The phosphorylation of IWS1 attracts SetD2 to the Spt6/IWS1/Aly complex in the CTD of RNA Pol II. SetD2 in the complex trimethylates histone H3 at K36 during transcriptional elongation. MRG15 and its partner PTB bind histone H3K36me3. Binding of PTB to the IIIb exon promotes exclusion of this exon from the spliced transcript.

phosphorylation of IWS1 plays a major role in the regulation of *FGFR-2* alternative splicing in primary human NSCLCs and are consistent with our other data showing that the knockdown of Akt1 and Akt3 shifts the splicing of FGFR-2 from the IIIc to the IIIb isoform. Since a low IIIb/IIIc ratio has been shown to promote EMT and tumor cell invasiveness (Thiery and Sleeman, 2006), these data support the hypothesis that Akt promotes cancer progression by phosphorylating IWS1. This conclusion is further supported by data from the oncomine database (Bild et al., 2006), which reveal a positive correlation between IWS1 expression with tumor stage (Figure S6C).

DISCUSSION

Linking Functional Differences between Akt Isoforms to Differences in Target Specificity

In this paper we focused on a phosphoproteomics screen, which was carried out in a set of lung fibroblast cell lines that express different Akt isoforms but are otherwise identical. The results revealed significant differences in target specificity between Akt isoforms and identified a host of signaling pathways and cellular functions that may be differentially regulated by them (Figure 2A). Some of the predictions, such as the regulation of insulin and IGF signaling primarily by Akt2, are in agreement with prior literature

(Cho et al., 2001). Based on these data it is expected that Akt inhibitors may have widely variable therapeutic effects and toxicity, depending on their relative specificity against the three Akt isoforms.

Regulation of RNA Processing by Akt Isoforms

One of the top functions differentially regulated by Akt isoforms is RNA metabolism, with 25 proteins involved in various steps of the RNA maturation process being phosphorylated by at least one of the three isoforms (Figures 2B and 2C). IWS1, one of these proteins, is phosphorylated primarily by Akt3 and Akt1 and is a component of a transcriptional elongation complex, which includes Spt6, Aly/REF, and SetD2 and assembles on the Ser2 phosphorylated CTD of RNA Pol II (Yoh et al., 2007, 2008). Data in this report showed that IWS1 phosphorylation is required for the recruitment of SetD2 to the complex and the trimethylation of histone H3 at K36 in the body of the target genes. Subsequent recruitment of the histone H3K36me3-intracting protein MRG15 and its binding partner PTB results in shifts in the alternative splicing of target genes, one of which is *FGFR-2*.

Regulation of Alternative RNA Splicing by Akt Isoforms

The alternative splicing of *FGFR-2* gives rise to two isoforms, IIIb and IIIc (Carstens et al., 2000; Warzecha et al., 2009). IIIb is expressed primarily in epithelial cells, while IIIc, which is the isoform induced by IWS1 phosphorylation, is expressed primarily

IIIc ratio was measured by quantitative RT-PCR. Bars show the ratio in cells treated with MK2206 relative to cells treated with DMSO (mean ±SD). p values were calculated with the Student's t test. (Bottom) ChIP assays measuring the abundance of H3K36me3 trimethylation in *FGFR-2* in the indicated cell lines before and after a 2 hr treatment with 5 μM MK2206 or with DMSO. Bars show the fold enrichment of the abundance of H3K36me3 trimethylation in DMSO-treated versus Akt inhibitor-treated cells (mean ±SD).

(D) The knockdown of Akt1 and/or Akt3 promotes inclusion of the IIIb exon in the *FGFR-2* transcript. Lysates of NCI H1299 cells harvested 48 hr after transfection with siAKT1, siAkt2, siAkt3, or siControl were probed with the indicated antibodies (left). IIIb/IIIc ratios were measured by quantitative RT-PCR (right). Bars show the IIIb/IIIc ratio in siAkt versus si-control cells (mean ±SD).

(E) The Akt-independent mutant IWS1-DE reversed the MK2206-induced shift in *FGFR-2* alternative splicing. RNA isolated from MK2206 or DMSO-treated NCI H522 and NCI H1299 cells transduced with the IWS1 phosphomimetic mutant IWS1-DE or the empty vector was analyzed for the IIIb/IIIc ratio by quantitative RT-PCR. Bars show the IIIb/IIIc ratio in MK2206-treated versus DMSO-treated cells (mean ±SD).

(F) *FGFR-2* splicing shifts toward the IIIc transcript in response to IGF1. RNA from the cells in Figure 3A was analyzed for the IIIb/IIIc ratio by quantitative RT-PCR. Bars show the IIIb/IIIc ratio in IGF1-treated versus untreated cells (mean ±SD).

(G and H) IWS1 phosphorylation is required for the binding of MRG15 to *FGFR-2*. ChIP assays showing the binding of MRG15 to the indicated sites in the *FGFR-2* and *GAPDH* genes in shControl, shIWS1, shIWS1/WT rescue, and shIWS1/mutant rescue NCI H522 (G) and NCI H1299 (H) cells. Bars show the mean fold enrichment in MRG15 binding in shControl versus shIWS1 or in shIWS1/WT rescue versus shIWS1/mutant rescue cells ±SD.

(I and J) IWS1 phosphorylation is required for the binding of PTB to *FGFR-2*. ChIP assays showing the binding of myc-PTB to the indicated sites in the *FGFR-2* and *GAPDH* genes in shControl, shIWS1, shIWS1/WT rescue, and shIWS1/mutant rescue NCI H522 (I) and NCI H1299 (J) cells, transfected with a myc-PTB construct. The expression of myc-PTB is shown in Figure S4E. Bars show the mean fold enrichment in myc-PTB binding in shControl versus shIWS1 or in shIWS1/WT rescue versus shIWS1/mutant rescue cells ±SD. Myc-PTB binding is also presented as percentage of the input in Figure S4E.
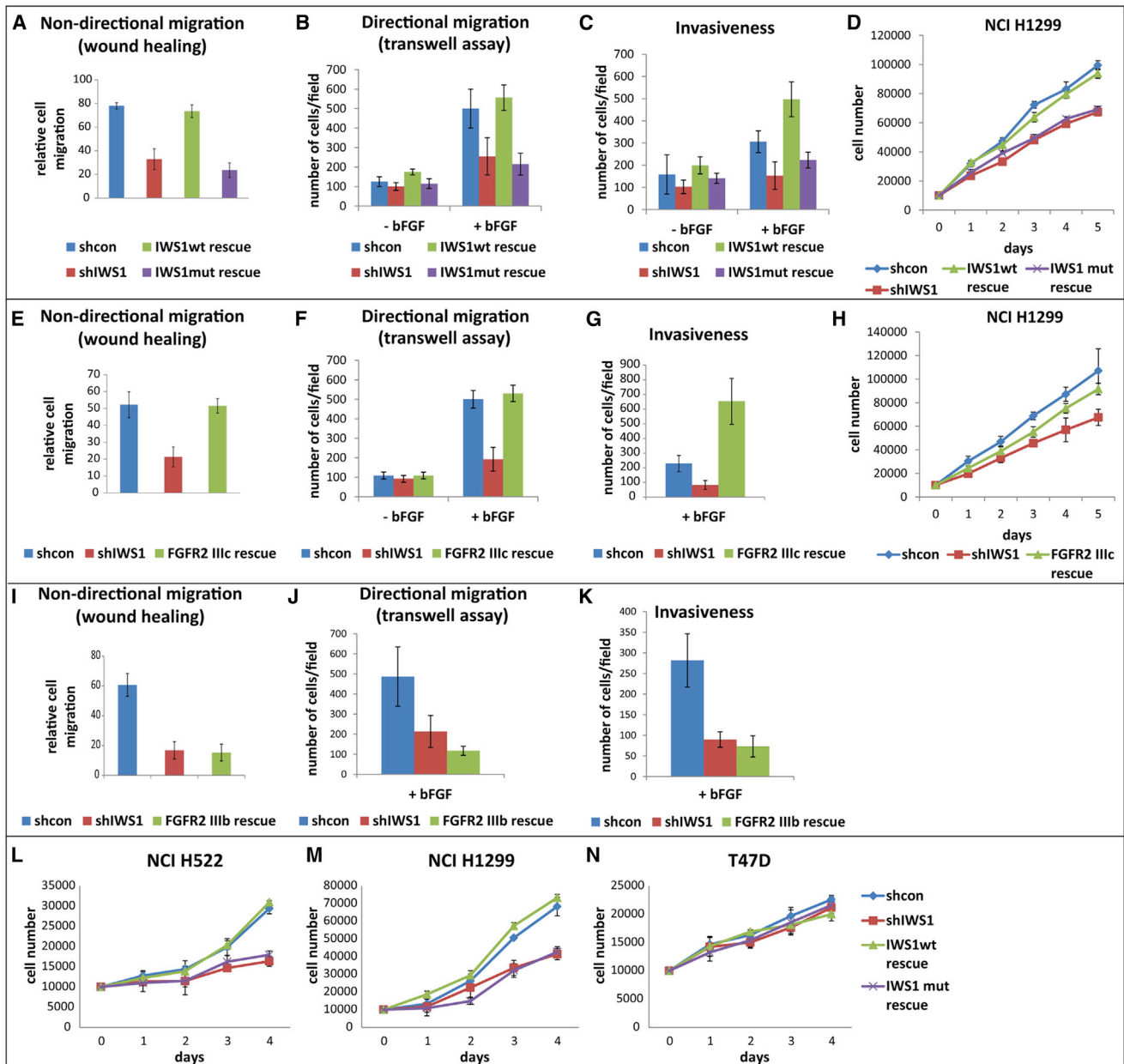
Figure 6. IWS1 Phosphorylation at Ser720/Thr721 in Lung Carcinoma Cell Lines Promotes Cell Migration, Invasiveness, and Proliferation

(A) Wound healing in serum-free media supplemented with FGF-2. Assays were carried out on confluent monolayers of the indicated NCI H1299 cells. The bars show the fraction of the width of the wound that was covered by the migrating cells 24 hr later (mean ±SD).

(B) Directional migration of the cells in (A) toward FGF-2 was measured with the transwell assay. Bars show the numbers of migrating cells (mean ±SD) at 16 hr.

(C) Cell invasiveness of the cells in (A) in FGF-2-free and FGF-2-containing semisolid media. Bars show the numbers of invading cells (mean ±SD) at 16 hr.

(D) Growth curves of the cells in (A), in media supplemented with 1% FBS and 20 ng/ml FGF-2. Live-cell numbers (mean ±SD) were measured with the MTT assay in five independent cultures of each cell type.

(E–G) The IIIc isoform of *FGFR-2* rescued the cell migration (E and F) and invasiveness (G) defects in shIWS1 NCI H1299 cells. Data are presented as in (A)–(C).

(H) Growth curves of the cells in (E), in media supplemented with 1% FBS and 20 ng/ml FGF-2. Live-cell numbers (mean ±SD) were measured with the MTT assay in five independent cultures of each cell type.

(I–K) The IIIb isoform of *FGFR-2* failed to rescue the cell migration (I and J) and invasiveness (K) defects in shIWS1 NCI H1299 cells. Data are presented as in (A)–(C).

(L–N) Growth curves of the indicated NCI H522, NCI H1299, and T47D cells in media supplemented with 10% FBS. Live-cell numbers (mean ±SD) were measured with the MTT assay in five independent cultures for each cell type.
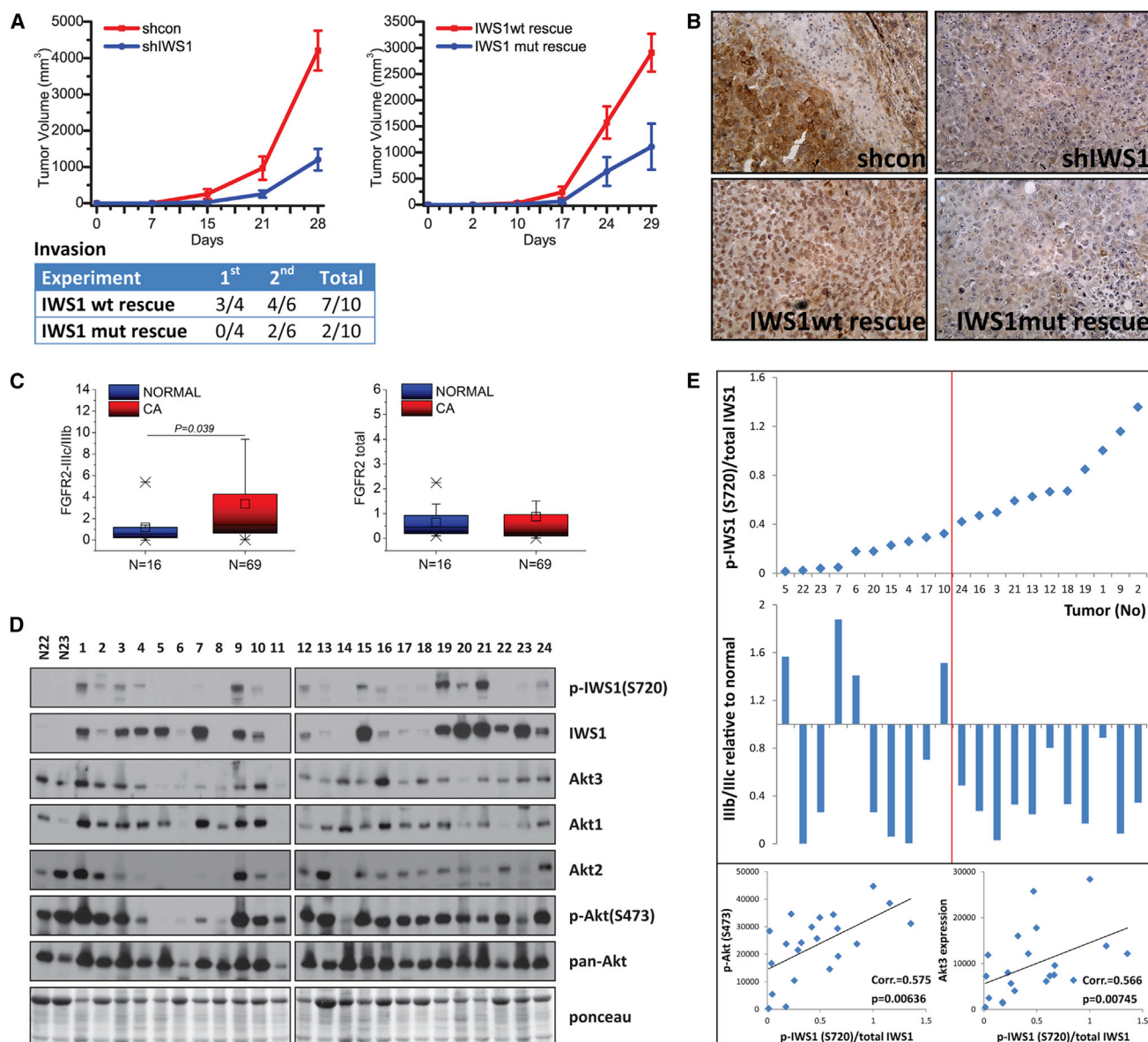
Figure 7. IWS1 Phosphorylation at Ser720/Thr721 in NSCLC

(A) IWS1 phosphorylation at Ser720/Thr721 promotes tumor growth and invasiveness in a xenograft NSCLC model in nude mice. Nude mice were injected subcutaneously with shControl, shIWS1, shIWS1/WT rescue, and shIWS1/mutant rescue NCI H1299 cells (n = 10 mice/group). (Top) Tumor growth is expressed as mean tumor volume ±SE. (Bottom) Frequency of macroscopic invasion of the adjacent tissue by the tumor cells. Shown are combined data from two experiments.

(B) Phospho-IWS1 (Ser720) staining of tumor xenografts. Formalin-fixed, paraffin-embedded tumor samples from the experiment in (A) were stained with a noncommercially available anti-phospho-IWS1 (Ser720) antibody from Cell Signaling (see Figure 3C, lower panel, and Figure S3B). Secondary antibody was HRP labeled. Tissues were counterstained with hematoxylin.

(C) *FGFR-2* IIIc/IIIb exon ratio (left) and *FGFR-2* expression (right) in normal human lung and lung cancer specimens were determined by quantitative RT-PCR and presented as box plots.

(D and E) The shift of *FGFR-2* splicing toward IIIc in NSCLCs correlates with IWS1 phosphorylation at Ser720/Thr721, and the latter correlates with Akt phosphorylation and Akt3 expression. (D) Lysates of 2 normal lung and 24 NSCLC samples were probed with the indicated antibodies. (E) (Upper) The relative stoichiometry of IWS1 phosphorylation in the 21 NSCLCs expressing IWS1 was estimated from the phospho-IWS1/total IWS1 band density ratios and was used to place the tumors in an ascending order of IWS1 phosphorylation abundance. (Middle) IIIb/IIIc exon ratios in the tumors in the upper panel. The IIIb/IIIc ratio in normal lung was given the value of 1. Bars show the ratios in tumors versus normal lung, with some tumors exhibiting values greater and some lower than 1. (Lower) The relative stoichiometry of IWS1 phosphorylation in the same tumors correlates with phospho-Akt (Ser473) (left) and Akt3 expression (right).

in mesenchymal cells and in invasive and metastatic tumors (Luco et al., 2010; Orr-Urtreger et al., 1993). Of these isoforms, only IIIc is recognized by FGF-2 (Miki et al., 1992). In agreement with these data, lung carcinoma cell lines in which the endogenous IWS1 was replaced with the phosphorylation site mutant exhibit defects in FGF-2-induced cell proliferation, migration, and invasion. More importantly, the defects in cell migration and invasiveness were fully rescued by *FGFR-2* IIIc, but not IIIb, while the defect in cell proliferation was rescued partially and only when the cells were grown in FGF-2-supplemented media. IWS1 phosphorylation and SetD2 recruitment are expected to target more genes, in addition to *FGFR-2* (Luco et al., 2010). Moreover, in some of these genes they may promote transcriptional elongation by preventing cryptic intragenic transcription, with or without an effect on RNA splicing (Carvalho et al., 2013). Based on these considerations, we propose that IWS1 phosphorylation may promote tumor cell proliferation in culture and in animals by regulating RNA splicing, transcriptional elongation, or both on a host of cellular genes.

It has been firmly established that splicing occurs cotranscriptionally and that it is influenced by the imprinting of the pre-mRNA, during the RNA synthesis and processing steps that precede splicing (Moore and Proudfoot, 2009). To explain how the process of transcription may affect splicing, two models have been proposed: the kinetic model, which suggests that slowing the rate of transcription promotes the inclusion of weak exons into the mature mRNA product, and the chromatin modification model, which proposes that histone and DNA modifications regulate the assembly of protein complexes that control splicing (Luco et al., 2011), although they may also control nucleosome density and the rate of transcriptional elongation.

Our data support the chromatin modification model (Figure 5), and they show how the chromatin-regulated RNA splicing machinery is under the control of Akt signals. However, the link between chromatin modifications and alternative splicing may be more complex than the model indicates. This is suggested by the following observations. In mesenchymal cells, which express the IIIc isoform of *FGFR-2*, histone H3 trimethylation at K36 is accompanied by the downregulation of histone H3K4 and H3K27 trimethylation, and by histone H3K4 mono- and dimethylation (Luco et al., 2010). More importantly, overexpression of the histone H3K4 methyltransferase ASH2 in these cells increases the usage of the normally repressed exon IIIb, suggesting that H3K4 trimethylation may also contribute to the regulation of PTB-dependent alternative splicing (Luco et al., 2010). Other studies provided evidence linking MRG15 to the acetylation of histone H4 at K16 (Conrad et al., 2012) and perhaps K12 (Peña et al., 2011) during transcriptional elongation. MRG15 is a component of several chromatin-modifying complexes, which could give rise to these chromatin modifications. Thus, it has been shown that MRG15 bound to the H3K36me3 mark in the body of transcribed genes (Zhang et al., 2006) also interacts with the histone H3K4me3/me2 demethylase KDM5B (Xie et al., 2011), the histone H4K16 acetyltransferase complex NuA4 (mammalian Tip60) (Cai et al., 2003), the histone H4K16 deacetylase complex Rpd3S (mammalian HDCA2) (Kumar et al., 2011), and VEZF1 (Gowher et al., 2012), a known regulator of alternative splicing. Some of these interactions may take place in the context of larger complexes, such as the LAF and RLAF complexes (Moshkin et al., 2009). It has not been determined yet whether these histone modifications are also observed in the context of the Akt3/Akt1-dependent shift in the alternative splicing of *FGFR-2*. If they do, the system we established will allow us to determine whether they play an obligatory role in this process, and to address the epistatic relationships between them.

Relevance of IWS1 Phosphorylation in Lung Cancer

It is now universally accepted that Akt plays a major role in oncogenesis. Experiments, both in culture and in animals, presented in this report revealed that IWS1 phosphorylation by Akt3 and Akt1 regulates RNA splicing and perhaps transcriptional elongation and represents an important event in lung cancer. Analysis of sets of normal lung and lung cancer samples for the expression of *FGFR-2* revealed that the overall expression is similar in both. However, the expression was shifted toward the IIIc isoform in the tumor samples. More importantly, the shift toward the IIIc isoform was found to correlate with the stoichiometry of IWS1 phosphorylation, which in turn correlates with Akt phosphorylation and Akt3 expression. Overall, this study identifies perturbations in RNA splicing and perhaps transcriptional elongation as a mechanism by which Akt promotes oncogenesis, shows that Akt isoforms contribute to oncogenesis as upstream regulators of FGF-2 signaling, and provides direct evidence linking IWS1 to lung cancer.

In summary, data presented in this report link Akt isoform-specific signaling with chromatin modifications occurring in the body of the gene encoding *FGFR-2*, and perhaps other actively transcribed target genes. These chromatin modifications, in turn, regulate alternative splicing and transcriptional elongation. By regulating these processes, IWS1 phosphorylation profoundly alters the biology of tumor cells. Interruption of IWS1 phosphorylation suppresses the proliferation, migration, and invasiveness of tumor cells both in culture and in animals. Overall, this study provides new insights into the regulation of alternative splicing, a process that plays a critical role in differentiation and development and in a multitude of human diseases, including cancer.

EXPERIMENTAL PROCEDURES

For details, see the Supplemental Information.

Cells, Culture, Growth Factors, and Akt Inhibitors
Mouse lung fibroblasts were described previously (Iliopoulos et al., 2009). Culture conditions, cell transfections, and infections are described in the Supplemental Information.

Phosphoproteomics Screen and Data Analysis
The phosphoproteomics screen and data analysis are presented in the Supplemental Information. Data are available at https://tuftsmedicalcenter. resultsbuilderstage.com/Research-Clinical-Trials/Institutes-Centers-Labs/ Molecular-Oncology-Research-Institute/Labs-Facilities/Tsichlis-Lab/Akt-phopshoproteomics.aspx.

siRNAs, shRNAs, and Expression Constructs, and Cloning and Site-Directed Mutagenesis
The origin of the siRNAs, shRNAs, and expression constructs is described in Table S3. Cloning and site-directed mutagenesis were carried out using standard procedures.

Immunoprecipitation, Immunoblotting, and In Vitro Kinase Assays

Immunoprecipitation, immunoblotting, and in vitro kinase assays are described in the Supplemental Information. The phosphorylation substrates (IWS1/WT and IWS1S720A/T721A) were expressed as GST fusions in *E. coli*, BL21. GSK3α/β was purchased from Cell Signaling Technology.

Real-Time RT-PCR

cDNA was synthesized from 1.0 μg of Trizol-extracted total cell RNA, using oligo-dT priming and the Retroscript reverse transcription kit from Ambion. Gene expression was quantified by real-time RT-PCR.

Chromatin Immunoprecipitation

ChIP assays, using the Millipore kit (catalog number 17-295), were done as described in the Supplemental Information.

Cell Proliferation, Migration, and Invasion Assays

Cell proliferation was monitored with the 3-(4,5-dimethylthiazol-2-yl)-2,5-diphenyltetrazolium bromide (MTT) assay. Nondirectional migration was measured with the wound-healing assay and directional migration with the transwell filter assay (Kottakis et al., 2011). In vitro invasion was measured using BD BioCoat Matrigel Invasion Chambers (BD Biosciences).

Tumor Xenografts

Nude mice injected subcutaneously with 2×10^6 shControl, shIWS1, shIWS1/WT rescue, or shIWS1mut rescue NCI H1299 cells were monitored for a total of 4 weeks.

Immunohistochemistry

A human lung tumor tissue array and xenograft tumors were stained with the specific anti-phospho-IWS1 (Ser720) antibody as described in the Supplemental Information.

REFERENCES

Bild, A.H., Yao, G., Chang, J.T., Wang, Q., Potti, A., Chasse, D., Joshi, M.B., Harpole, D., Lancaster, J.M., Berchuck, A., et al. (2006). Oncogenic pathway signatures in human cancers as a guide to targeted therapies. Nature *439*, 353–357.

Cai, Y., Jin, J., Tomomori-Sato, C., Sato, S., Sorokina, I., Parmely, T.J., Conaway, R.C., and Conaway, J.W. (2003). Identification of new subunits of the multiprotein mammalian TRRAP/TIP60-containing histone acetyltransferase complex. J. Biol. Chem. *278*, 42733–42736.

Carstens, R.P., Wagner, E.J., and Garcia-Blanco, M.A. (2000). An intronic splicing silencer causes skipping of the IIIb exon of fibroblast growth factor receptor 2 through involvement of polypyrimidine tract binding protein. Mol. Cell. Biol. *20*, 7388–7400.

Carvalho, S., Raposo, A.C., Martins, F.B., Grosso, A.R., Sridhara, S.C., Rino, J., Carmo-Fonseca, M., and de Almeida, S.F. (2013). Histone methyltransferase SETD2 coordinates FACT recruitment with nucleosome dynamics during transcription. Nucleic Acids Res. *41*, 2881–2893.

Chen, M., and Manley, J.L. (2009). Mechanisms of alternative splicing regulation: insights from molecular and genomics approaches. Nat. Rev. Mol. Cell Biol. *10*, 741–754.

Chen, W.S., Xu, P.Z., Gottlob, K., Chen, M.L., Sokol, K., Shiyanova, T., Roninson, I., Weng, W., Suzuki, R., Tobe, K., et al. (2001). Growth retardation and increased apoptosis in mice with homozygous disruption of the Akt1 gene. Genes Dev. *15*, 2203–2208.

Cho, H., Mu, J., Kim, J.K., Thorvaldsen, J.L., Chu, Q., Crenshaw, E.B., 3rd, Kaestner, K.H., Bartolomei, M.S., Shulman, G.I., and Birnbaum, M.J. (2001). Insulin resistance and a diabetes mellitus-like syndrome in mice lacking the protein kinase Akt2 (PKB beta). Science *292*, 1728–1731.

Conrad, T., Cavalli, F.M., Holz, H., Hallacli, E., Kind, J., Ilik, I., Vaquerizas, J.M., Luscombe, N.M., and Akhtar, A. (2012). The MOF chromobarrel domain controls genome-wide H4K16 acetylation and spreading of the MSL complex. Dev. Cell *22*, 610–624.

Cooper, T.A., Wan, L., and Dreyfuss, G. (2009). RNA and disease. Cell *136*, 777–793.

Duina, A.A. (2011). Histone chaperones Spt6 and FACT: similarities and differences in modes of action at transcribed genes. Genet. Res. Int. *2011*, 625210.

Ezell, S.A., Polytarchou, C., Hatziapostolou, M., Guo, A., Sanidas, I., Bihani, T., Comb, M.J., Sourvinos, G., and Tsichlis, P.N. (2012). The protein kinase Akt1 regulates the interferon response through phosphorylation of the transcriptional repressor EMSY. Proc. Natl. Acad. Sci. USA *109*, E613–E621.

Franke, T.F., Yang, S.I., Chan, T.O., Datta, K., Kazlauskas, A., Morrison, D.K., Kaplan, D.R., and Tsichlis, P.N. (1995). The protein kinase encoded by the Akt proto-oncogene is a target of the PDGF-activated phosphatidylinositol 3-kinase. Cell *81*, 727–736.

Gowher, H., Brick, K., Camerini-Otero, R.D., and Felsenfeld, G. (2012). Vezf1 protein binding sites genome-wide are associated with pausing of elongating RNA polymerase II. Proc. Natl. Acad. Sci. USA *109*, 2370–2375.

Iliopoulos, D., Polytarchou, C., Hatziapostolou, M., Kottakis, F., Maroulakou, I.G., Struhl, K., and Tsichlis, P.N. (2009). MicroRNAs differentially regulated by Akt isoforms control EMT and stem cell renewal in cancer cells. Sci. Signal. *2*, ra62.

Kalsotra, A., and Cooper, T.A. (2011). Functional consequences of developmentally regulated alternative splicing. Nat. Rev. Genet. *12*, 715–729.

Kolasinska-Zwierz, P., Down, T., Latorre, I., Liu, T., Liu, X.S., and Ahringer, J. (2009). Differential chromatin marking of introns and expressed exons by H3K36me3. Nat. Genet. *41*, 376–381.

Kottakis, F., Polytarchou, C., Foltopoulou, P., Sanidas, I., Kampranis, S.C., and Tsichlis, P.N. (2011). FGF-2 regulates cell proliferation, migration, and angiogenesis through an NDY1/KDM2B-miR-101-EZH2 pathway. Mol. Cell *43*, 285–298.

Krogan, N.J., Kim, M., Ahn, S.H., Zhong, G., Kobor, M.S., Cagney, G., Emili, A., Shilatifard, A., Buratowski, S., and Greenblatt, J.F. (2002). RNA polymerase II elongation factors of Saccharomyces cerevisiae: a targeted proteomics approach. Mol. Cell. Biol. *22*, 6979–6992.

Kumar, G.S., Xie, T., Zhang, Y., and Radhakrishnan, I. (2011). Solution structure of the mSin3A PAH2-Pf1 SID1 complex: a Mad1/Mxd1-like interaction disrupted by MRG15 in the Rpd3S/Sin3S complex. J. Mol. Biol. *408*, 987–1000.

Luco, R.F., Pan, Q., Tominaga, K., Blencowe, B.J., Pereira-Smith, O.M., and Misteli, T. (2010). Regulation of alternative splicing by histone modifications. Science 327, 996–1000.

Luco, R.F., Allo, M., Schor, I.E., Kornblihtt, A.R., and Misteli, T. (2011). Epigenetics in alternative pre-mRNA splicing. Cell 144, 16–26.

Manning, B.D., and Cantley, L.C. (2007). AKT/PKB signaling: navigating downstream. Cell 129, 1261–1274.

Maroulakou, I.G., Oemler, W., Naber, S.P., and Tsichlis, P.N. (2007). Akt1 ablation inhibits, whereas Akt2 ablation accelerates, the development of mammary adenocarcinomas in mouse mammary tumor virus (MMTV)-ErbB2/neu and MMTV-polyoma middle T transgenic mice. Cancer Res. 67, 167–177.

Miki, T., Bottaro, D.P., Fleming, T.P., Smith, C.L., Burgess, W.H., Chan, A.M., and Aaronson, S.A. (1992). Determination of ligand-binding specificity by alternative splicing: two distinct growth factor receptors encoded by a single gene. Proc. Natl. Acad. Sci. USA 89, 246–250.

Moore, M.J., and Proudfoot, N.J. (2009). Pre-mRNA processing reaches back to transcription and ahead to translation. Cell 136, 688–700.

Moshkin, Y.M., Kan, T.W., Goodfellow, H., Bezstarosti, K., Maeda, R.K., Pilyugin, M., Karch, F., Bray, S.J., Demmers, J.A., and Verrijzer, C.P. (2009). Histone chaperones ASF1 and NAP1 differentially modulate removal of active histone marks by LID-RPD3 complexes during NOTCH silencing. Mol. Cell 35, 782–793.

Orr-Urtreger, A., Bedford, M.T., Burakova, T., Arman, E., Zimmer, Y., Yayon, A., Givol, D., and Lonai, P. (1993). Developmental localization of the splicing alternatives of fibroblast growth factor receptor-2 (FGFR2). Dev. Biol. 158, 475–486.

Peña, A.N., Tominaga, K., and Pereira-Smith, O.M. (2011). MRG15 activates the cdc2 promoter via histone acetylation in human cells. Exp. Cell Res. 317, 1534–1540.

Polytarchou, C., Iliopoulos, D., Hatziapostolou, M., Kottakis, F., Maroulakou, I., Struhl, K., and Tsichlis, P.N. (2011). Akt2 regulates all Akt isoforms and promotes resistance to hypoxia through induction of miR-21 upon oxygen deprivation. Cancer Res. 71, 4720–4731.

Thiery, J.P., and Sleeman, J.P. (2006). Complex networks orchestrate epithelial-mesenchymal transitions. Nat. Rev. Mol. Cell Biol. 7, 131–142.

Tschopp, O., Yang, Z.Z., Brodbeck, D., Dummler, B.A., Hemmings-Mieszczak, M., Watanabe, T., Michaelis, T., Frahm, J., and Hemmings, B.A. (2005). Essential role of protein kinase B gamma (PKB gamma/Akt3) in postnatal brain development but not in glucose homeostasis. Development 132, 2943–2954.

Wan, M., Leavens, K.F., Saleh, D., Easton, R.M., Guertin, D.A., Peterson, T.R., Kaestner, K.H., Sabatini, D.M., and Birnbaum, M.J. (2011). Postprandial hepatic lipid metabolism requires signaling through Akt2 independent of the transcription factors FoxA2, FoxO1, and SREBP1c. Cell Metab. 14, 516–527.

Wang, E.T., Sandberg, R., Luo, S., Khrebtukova, I., Zhang, L., Mayr, C., Kingsmore, S.F., Schroth, G.P., and Burge, C.B. (2008). Alternative isoform regulation in human tissue transcriptomes. Nature 456, 470–476.

Warzecha, C.C., Sato, T.K., Nabet, B., Hogenesch, J.B., and Carstens, R.P. (2009). ESRP1 and ESRP2 are epithelial cell-type-specific regulators of FGFR2 splicing. Mol. Cell 33, 591–601.

Xie, L., Pelz, C., Wang, W., Bashar, A., Varlamova, O., Shadle, S., and Impey, S. (2011). KDM5B regulates embryonic stem cell self-renewal and represses cryptic intragenic transcription. EMBO J. 30, 1473–1484.

Yoh, S.M., Cho, H., Pickle, L., Evans, R.M., and Jones, K.A. (2007). The Spt6 SH2 domain binds Ser2-P RNAPII to direct Iws1-dependent mRNA splicing and export. Genes Dev. 21, 160–174.

Yoh, S.M., Lucas, J.S., and Jones, K.A. (2008). The Iws1:Spt6:CTD complex controls cotranscriptional mRNA biosynthesis and HYPB/Setd2-mediated histone H3K36 methylation. Genes Dev. 22, 3422–3434.

Zhang, P., Du, J., Sun, B., Dong, X., Xu, G., Zhou, J., Huang, Q., Liu, Q., Hao, Q., and Ding, J. (2006). Structure of human MRG15 chromo domain and its binding to Lys36-methylated histone H3. Nucleic Acids Res. 34, 6621–6628.

Zhou, Z., Qiu, J., Liu, W., Zhou, Y., Plocinik, R.M., Li, H., Hu, Q., Ghosh, G., Adams, J.A., Rosenfeld, M.G., and Fu, X.D. (2012). The Akt-SRPK-SR axis constitutes a major pathway in transducing EGF signaling to regulate alternative splicing in the nucleus. Mol. Cell 47, 422–433.